Computed tomography and low-field magnetic resonance imaging of the pituitary gland in dogs with pituitary-dependent hyperadrenocorticism: 11 cases (2001–2003)

Edoardo Auriemma, DVM; Paul Y. Barthez, DVM, PhD; Roselinda H. van der Vlugt-Meijer, DVM, PhD; George Voorhout, DVM, PhD; Björn P. Meij, DVM, PhD

Objective—To compare the results of computed tomography (CT) and magnetic resonance imaging (MRI) of the pituitary gland in dogs with pituitary-dependent hyperadrenocorticism (PDH) caused by histologically confirmed pituitary adenoma.

Design—Retrospective case series.

Animals—11 dogs with PDH that underwent transsphenoidal hypophysectomy.

Procedures—Medical records of dogs examined between January 2001 and March 2003 were reviewed. Dogs were included in this study if they had clinical signs of hypercortisolism at the time of admission (for which PDH was diagnosed) and underwent transsphenoidal hypophysectomy. Pre- and postcontrast CT and low-field MRI (0.2-Tesla magnet) were performed on the same day as surgery for each dog.

Results—An abnormal pituitary gland was found in 7 dogs by use of MRI and in the same 7 dogs by use of CT. Significant differences were found between postcontrast CT and MR images for height, width, and length of the pituitary gland; brain area; and thickness of the sphenoid bone. However, the pituitary gland height-to-brain area ratio determined from postcontrast CT and MR images was not significantly different. The signal-to-noise ratio and contrast-to-noise ratio of pre- and postcontrast MR images were significantly higher than those of the CT images.

Conclusions and Clinical Relevance—Low-field MRI and dynamic CT imaging of the pituitary gland provided comparable information on the presence of pituitary adenomas in dogs with PDH. (*J Am Vet Med Assoc* 2009;235:409–414)

Computed tomography has been used routinely in the diagnosis and presurgical evaluation of dogs with PDH.[1–5] Computed tomography performed after IV injection of iodinated contrast medium provides information on the size of the pituitary gland and its location relative to the bony surgical landmarks that are required for surgical intervention.[6,7] When conventional postcontrast CT images are not sufficient to detect changes compatible with an adenoma (such as in microadenoma), dynamic CT of the pituitary gland can reveal the site of the microadenoma by detecting distortion of the neurohypophyseal flush.[1]

Conventional and dynamic MRI of healthy dogs[8–10] and of dogs affected by large pituitary tumors[11,12] has been reported. Magnetic resonance imaging of the pituitary gland is the technique of choice in humans with pituitary disease, but detection of pituitary lesions depends on the use of high-field MRI with 1.5- to 3.0-Tesla closed MRI machines.[13,14] Even with these high-field MRI machines, detection of a pituitary microadenoma that is < 2 mm in diameter remains a problem. Therefore, it is unclear as to which modality, CT or low-field MRI, should be chosen for imaging the pituitary gland in dogs with PDH. The purpose of the study reported here was to compare the results of conventional and dynamic CT with those of low-field (0.2-Tesla) MRI of the pituitary gland in dogs with PDH caused by histologically confirmed pituitary adenoma.

Abbreviations

CNRpg-b	Contrast-to-noise ratio of the pituitary gland in relation to the brain
CT	Computed tomography
MR	Magnetic resonance
MRI	Magnetic resonance imaging
P:B ratio	Pituitary gland height-to-brain area ratio
PDH	Pituitary-dependent hyperadrenocorticism
SNRb	Signal-to-noise ratio of the brain
SNRpg	Signal-to-noise ratio of the pituitary gland

Materials and Methods

Criteria for case selection—Medical records were reviewed of dogs examined at the veterinary hospi-

From the Division of Diagnostic Imaging (Auriemma) and the Department of Clinical Sciences of Companion Animals (Barthez, van der Vlugt-Meijer, Voorhout, Meij), Faculty of Veterinary Medicine, Utrecht University, 3508 TC Utrecht, The Netherlands. Dr. Barthez's present address is VEDIM, Route de Luxembourg 76, L-4972 Dippach, Luxembourg, Luxembourg. Dr. van der Vlugt-Meijer's present address is ACE Pharmaceuticals BV, PO Box 1262, 3980 BB Zeewolde, The Netherlands.

Address correspondence to Dr. Auriemma.

tal of Utrecht University between January 2001 and March 2003. Dogs were included in this study if they met the following criteria: had clinical signs of hypercortisolism at the time of admission (for which PDH was diagnosed) and underwent transsphenoidal hypophysectomy at our institution.[15] Eleven dogs (1 Shar Pei, 2 Malteses, 1 Dachshund, 2 Boxers, 1 Schnauzer, 1 Alaskan Malamute, 1 West Highland White Terrier, and 2 mixed-breed dogs) were included. Dogs (2 sexually intact females, 4 castrated females, 4 sexually intact males, and 1 castrated male) had a median age of 9.2 years (range, 3.9 to 12.3 years) and median body weight of 25 kg (55.1 lb) that ranged from 7 to 61 kg (15.4 to 134.5 lb).

Diagnosis of PDH and hypophysectomy—Hypercortisolism was diagnosed by clinical signs, routine laboratory investigation, and determination of the urinary corticoid-to-creatinine ratio in 2 consecutive morning urine samples as described previously.[15–18] Mean corticoid-to-creatinine ratio was 96×10^{-6} (range, 10 to 383 $\times 10^{-6}$; reference limit, $< 10 \times 10^{-6}$).[19] After collection of the second urine sample, 3 doses of dexamethasone (0.1 mg/kg [0.05 mg/lb], PO) were administered at 8-hour intervals, and the next morning, a third urine sample was collected (high-dose dexamethasone suppression test).[19] In 10 dogs, the corticoid-to-creatinine ratio in the third sample was < 50% of the mean in the first 2 samples, and PDH was diagnosed. In 1 dog with < 50% suppression, dexamethasone-resistant PDH was confirmed by measurements of plasma ACTH concentrations and further supported by visualization of the adrenal glands on ultrasonographic examination of the pituitary gland.[4,20–22] Computed tomography and MRI were performed under anesthesia on the same day in all dogs. Transsphenoidal hypophysectomy was performed by a microsurgical technique that has been described previously.[6,7] In all dogs, the histologic examination of the pituitary gland tissue confirmed the diagnosis of pituitary adenoma.

Anesthesia for pituitary gland imaging—Food was withheld from dogs for 18 hours before CT or MRI. After administration of medetomidine (50 µg/kg [22.7 µg/lb], IV), anesthesia was induced by administration propofol (1 to 2 mg/kg [0.5 to 0.9 mg/lb], IV). The trachea was intubated, and inhalation anesthesia was maintained in a semiclosed system with a mixture of isoflurane, nitrous oxide, and oxygen.

CT—Computed tomography was performed with a third-generation CT scanner[a] with dogs in sternal recumbency. Precontrast, dynamic, and postcontrast CT images of the pituitary gland were obtained following a previously described protocol.[1] Transverse scans of the pituitary fossa were made as pre- and postcontrast images (9-second scanning time, 120 kV, 220 mA, and 2-mm-thick consecutive slices). For the dynamic scan, the largest cross-sectional image of the pituitary gland (usually just rostral to the dorsum sellae) was chosen, and at this position, a series of 2-mm-thick CT images was acquired by use of 4.5-second scanning time and 9.5-second interscan time.

One scan was made before contrast medium injection, and then a series of 8 to 10 scans (dynamic series of scan) was made during and after the IV bolus injection of a solution of sodium and meglumine ioxotalamate[b] (containing iodine [350 mg/mL]; maximum volume of 60 mL).

Because of a 5-second standby delay before the start of a series of scans (inherent to the scanner used), the first scan of this series was started 5 seconds after the start of the contrast medium injection. After the dynamic series, an additional bolus dose of 1 mL/kg of the same contrast medium was injected, and an additional series of 2-mm-thick consecutive images from the rostral clinoid processes to the dorsum sellae was acquired.

MRI—Magnetic resonance imaging was performed with a 0.2-Tesla open magnet[c] with dogs in sternal recumbency; a small multipurpose coil was used. Contrast medium[d] contained meglumine gadoterate (377 mg/mL) and was administered IV (0.2 mL/kg [0.09 mL/lb]). Contiguous 1-mm-thick slices of the pituitary gland were obtained by use of a pre- and postcontrast T1-weighted 3-D gradient echo sequence[10] (flash, 3-D; time of repetition, 34 milliseconds; time of echo, 12 milliseconds; slab thickness, 32 mm; time of acquisition, 22.02 minutes; rectangular field of view, 140 × 160 mm) and flip angle of 30°.

Image analysis—Pre- and postcontrast CT and MR images were analyzed by a single person (EA). On precontrast CT and MR images, the signal and the size and signal of the pituitary gland were evaluated, respectively. On postcontrast CT and MR images, the height, width, and length of the pituitary gland; the brain area; and the thickness of the basisphenoid bone were measured. The P:B ratio was calculated as the ratio of pituitary gland height (mm) to brain area (mm^2) × 100. Pituitary glands with a P:B ratio ≤ 0.31 were considered normal in size, and pituitary glands with a P:B ratio > 0.31 were considered enlarged.[5] On dynamic CT, the presence or absence of a pituitary flush and its position within the contours of the pituitary gland were assessed. On precontrast MR images, the detection of the pituitary bright signal was recorded, and its position inside the pituitary gland was determined. Quality of images was determined on pre- and postcontrast CT and MR images by calculating the SNRpg and SNRb. On the image that contained the largest cross section of the pituitary gland, regions of interests were selected representing the pituitary gland, the brain (including an area containing gray and white matter and no lateral ventricles), and the background (area outside the skull). The SNRpg and SNRb were calculated as the signal intensity of the pituitary gland or brain, respectively, divided by the SD of the background intensity. The CNRpg-b was calculated by subtraction of the SNRb from the SNRpg.[10]

Statistical analysis—The height, width, and length of the pituitary gland; the brain area; the P:B ratio; and the thickness of the basisphenoid bone were compared between postcontrast CT and MR images by use of a paired Student *t* test assuming normal distribution of the data. Nonparametric statistics (Friedman and Wilcoxon signed rank tests) were used to compare the SNRb and the SNRpg, the CNRpg-b between pre- and postcontrast CT images, and the CNRpg-b between pre- and postcontrast MR images. Significance was set at $P < 0.05$.

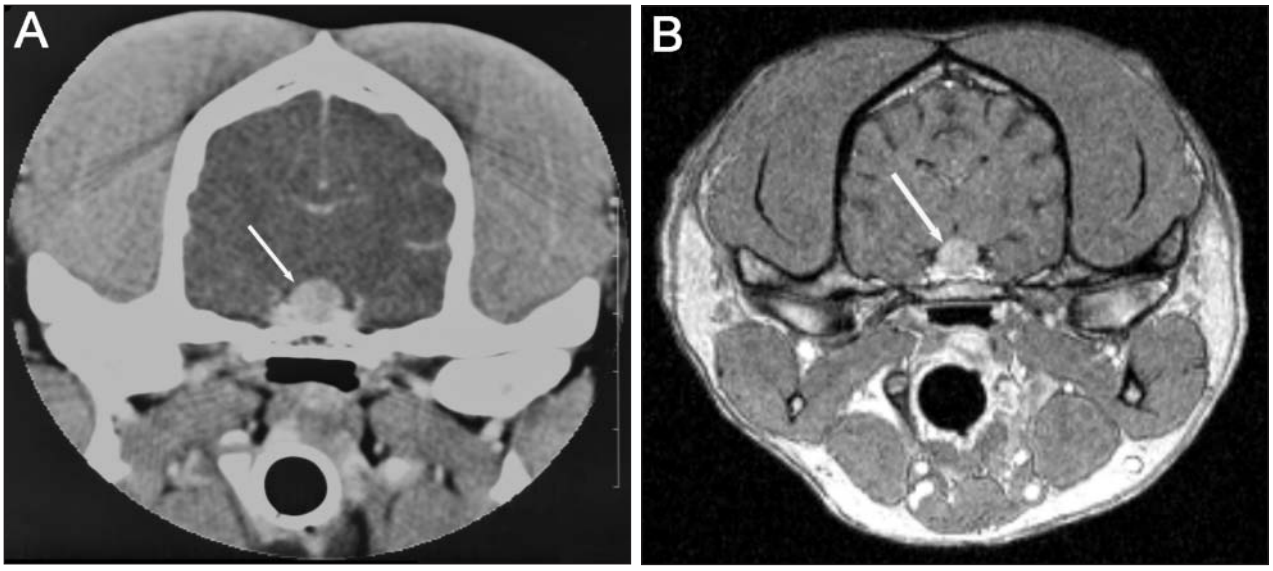

Figure 1—Transverse postcontrast CT (A) and postcontrast MR (B) images of the brain from a dog with PDH. The pituitary gland (arrow) is enlarged (P:B ratio = 0.53).

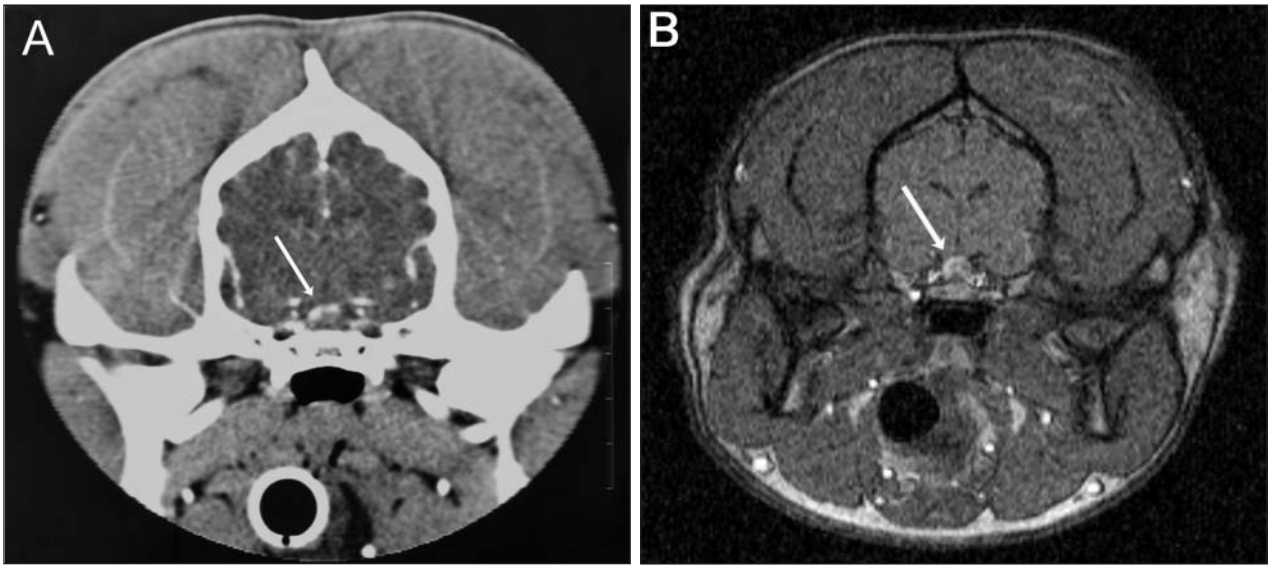

Figure 2—Transverse postcontrast CT (A) and precontrast MR (B) images of the brain from a dog with PDH. Notice the displacement of the pituitary flush (arrow) on dynamic CT and displacement of the bright spot (arrow) on precontrast T1-weighted MRI.

Results

In 4 dogs with PDH, the pituitary gland was not enlarged and had a normal pituitary flush on dynamic CT. In 7 dogs, the pituitary gland was enlarged with a P:B ratio > 0.31 on postcontrast CT images (**Figure 1**). In 3 of these 7 dogs, pituitary enlargement was already evident on precontrast CT images. On precontrast CT images, the pituitary gland was more attenuating than the surrounding brain in 2 dogs, less attenuating in 1 dog, and isoattenuating in 8 dogs. Displacement of the neurohypophyseal flush (**Figure 2**) was identified on dynamic CT in 2 dogs, and both dogs had a P:B ratio > 0.31.

Magnetic resonance imaging revealed a normal pituitary gland in 4 dogs, and these were the same dogs that had no abnormalities on CT. Abnormal findings were identified on MR images in the same 7 dogs that had abnormal findings on the CT images. A decreased signal intensity of the pituitary gland was seen on precontrast T1-weighted MR images in 2 dogs. On postcontrast images, 7 dogs had a P:B ratio > 0.31 (Figure 1). Displace-

Table 1—Mean ± SD dimensions of the pituitary gland (height, width, and length), brain area, P:B ratio, and sphenoid bone thickness on postcontrast CT and MR images in 11 dogs with PDH.

Dimension	Postcontrast CT	Postcontrast MRI	*P* value*
Height (mm)	7.30 ± 5.00	8.12 ± 5.13	< 0.001
Width (mm)	8.18 ± 4.65	8.66 ± 4.56	0.029
Length (mm)	7.64 ± 4.65	9.08 ± 4.79	0.014
Brain area (mm^2)	1,516.44 ± 177.32	1,796.57 ± 243.38	< 0.001
P:B ratio (mm^{-1})	0.44 ± 0.28	0.44 ± 0.23	0.906
Bone thickness (mm)	5.62 ± 1.77	4.19 ± 1.69	0.002

*Comparison between CT and MRI values by use of a paired Student *t* test.

Table 2—The SNRb, SNRpg, and CNRpg-b on pre- and postcontrast CT and MR images in 11 dogs with PDH.

Variable	Precontrast CT	Postcontrast CT	Precontrast MRI	Postcontrast MRI	*P* value*
SNRb	1.74 ± 1.88	2.04 ± 2.33	17.59 ± 8.69	16.66 ± 6.72	< 0.001
SNRpg	2.75 ± 3.37	4.47 ± 5.95	19.01 ± 12.56	22.04 ± 11.76	< 0.001
CNRpg-b	1.01 ± 1.80	2.42 ± 3.96	4.04 ± 5.15	7.04 ± 6.40	< 0.001

*Comparison between CT and MRI values by use of the Friedman test.

Table 3—*P* values from Wilcoxon signed rank testing of comparisons of the SNRb, SNRpg, and CNRpg-b on pre- and postcontrast CT and MR images in 11 dogs with PDH.

Variable	Postcontrast CT	Precontrast MRI	Postcontrast MRI
Precontrast CT			
SNRb	0.005	0.004	0.004
SNRpg	0.004	0.005	0.004
CNRpg-b	0.004	0.035	0.008
Postcontrast CT			
SNRb		0.004	0.004
SNRpg		0.014	0.005
CNRpg-b		0.490	0.043
Precontrast MR			
SNRb			0.675
SNRpg			0.066
CNRpg-b			0.017

ment of the bright spot on precontrast T1-weighted MR images was identified in 2 dogs, both with a P:B ratio > 0.31, including 1 dog with a decreased signal intensity of the pituitary gland. Dogs with a displaced bright spot on MRI were the same dogs that had a displaced neurohypophyseal flush on CT (Figure 2). Absence of the bright spot on precontrast T1-weighted MR images was detected in 5 dogs, of which 4 dogs had a P:B ratio > 0.31 and 1 had a P:B ratio < 0.31 on postcontrast MR images.

Significant differences were found between pituitary dimensions on postcontrast CT and MR images for pituitary height ($P = < 0.001$), width ($P = 0.029$), and length ($P = 0.014$); brain area ($P < 0.001$); and thickness of the sphenoid bone ($P = 0.002$; **Table 1**). However, the P:B ratio determined from postcontrast CT and MR images was not significantly different.

Significant differences were found in SNRb ($P < 0.001$), SNRpg ($P < 0.001$), and CNRpg-b ($P < 0.001$) on pre- and postcontrast CT and pre- and postcontrast MR images (**Table 2**). The SNRb and the SNRpg were significantly higher on pre- and postcontrast MR images than on pre- and postcontrast CT images. The SNRb and SNRpg were also significantly higher on postcontrast CT than on precontrast CT, but no significant differences were found in the SNRb and SNRpg between pre- and postcontrast MR images (**Table 3**).

The CNRpg-b on postcontrast CT images was not significantly ($P = 0.490$) different from the CNRpg-b on precontrast MR images, but was significantly ($P = 0.004$) higher than the CNRpg-b on precontrast CT and significantly ($P = 0.043$) lower than the CNRpg-b on postcontrast MR images (Table 2 and 3). The CNRpg-b was also significantly higher on pre- ($P = 0.035$) and postcontrast ($P = 0.008$) MR images than on precontrast CT images. The CNRpg-b of postcontrast MR images was significantly ($P = 0.017$) higher than the CNRpg-b of precontrast MR images.

Discussion

Results of the present study suggested that low-field MR and dynamic CT imaging of the pituitary gland can provide comparable information regarding the presence of pituitary adenomas. Results of this study confirmed that large pituitary tumors with changes in x-ray attenuation on CT images or signal intensity on MR images can be identified by use of the 2 modalities interchangeably.[11,12] Pituitary microadenomas, which do not change the size or shape of the pituitary gland, may be more challenging to identify with either of these 2 modalities. The main issues in the detection of small pituitary tumors are spatial and contrast resolution to detect subtle changes in size or signal intensity and determination of reference values to separate dogs with pituitary tumors from dogs with normal anatomic variation.

Spatial and contrast resolution of most modern CT units allow identification of abnormalities of the pituitary gland as small as 1 to 2 mm in diameter.[1] The value of postcontrast CT images to identify enlarged pituitary glands has been demonstrated.[5] The P:B ratio has been determined to be the best discriminative index to separate enlarged from nonenlarged pituitary glands.[5] Dynamic CT of the pituitary gland gives additional information by demonstration of displacement of the neurohypophysis without changes in pituitary gland size.[1] A combination of valuable information collected on the pituitary gland and logistic considerations has made, up to now, dynamic CT the modality of choice for the diagnosis and presurgical evaluation of pituitary tumors in our institution.[23]

Magnetic resonance imaging is the modality of choice for the evaluation of pituitary glands in humans, and its use has been advocated in dogs since the mid-1990s for the diagnosis of pituitary tumors as a result of its exquisite contrast resolution.[11] Results of our study indicated a better image quality (signal-to-noise ratio and contrast-to-noise ratio) of MR images, compared with CT images, even with a low-field MR unit. The diagnosis of small pituitary tumors on MRI, however, is influenced greatly by slice thickness.[10] Use of excessively thick slices (3 mm or more) may result in false-negative findings in dogs with small (1 or 2 mm in diameter) pituitary adenomas. In previous studies on MRI of the pituitary gland in healthy dogs[8,9] and in dogs with PDH,[11,12,24] a slice thickness of 3 mm or more was used, preventing identification of subtle anatomic changes in the pituitary fossa. Admittedly, maximal tumor detection was set at 3 mm in a study[24] involving dogs with PDH. In our dogs, thin (1- and 2-mm) slice gradient echo sequences were used to allow description of normal anatomic structures of the pituitary fossa.[10]

Use of MRI in the diagnosis of small pituitary tumors is impaired by the lack of a specific discriminative factor to separate enlarged from nonenlarged pituitary

glands. In 1 study,[11] 4 mm was taken as the cutoff value as height of the pituitary gland for the diagnosis of pituitary tumors. However, in another study[9] including a large number of dogs, the normal height of the pituitary gland was shown to average 5.1 mm and to be independent of the body size. Use of normalization to a body index (ie, brain area) has been demonstrated to improve discrimination between normal and abnormal pituitary gland on CT images and should therefore be recommended.[5] Comparison of the P:B ratio obtained on MR images in healthy dogs[10] and in the present study suggested that normal values of P:B ratio can be extrapolated reasonably from CT to MRI. The P:B ratio is influenced by measurement of the height of the pituitary gland and the brain area, both of which depend greatly on bony landmarks. Results of our study indicated that bony landmarks are slightly different in CT and MRI, resulting in different pituitary height and brain area, but a similar P:B ratio. It is our hypothesis that differences in pituitary height and brain area seen between CT and MR images equally affect each other in the calculation of the P:B ratio.

Significant differences between CT and MRI measurements for pituitary dimensions and sphenoid bone thickness found in the present study are inherent to the imaging characteristics of the 2 techniques (ie, CT has a focus on bone, and MRI has a focus on soft tissue). The surgeon should consider this difference between CT and MR images when assessing the pituitary dimensions and sphenoid bone thickness in the preoperative planning.

Additional information provided by dynamic CT in dogs with a nonenlarged pituitary gland is related to displacement of the neurohypophysis and is similar to changes of the bright spot detected on noncontrast T1-weighted MR images. Both the pituitary flush on dynamic CT and the bright spot on MR images represent the same anatomic structure (ie, the neurohypophysis, but a different physiologic phenomenon). The pituitary flush on dynamic CT images represents the early arterial blood supply of the neurohypophysis that is slightly earlier than the enhancement of the adenohypophysis through the portal blood supply. The bright spot on MR images also represents the neurohypophysis,[8,10] but appears to be related to vasopressin concentration in the pars distalis of the neurohypophysis.[25] The bright signal has been reported in 63% to 100% of healthy humans and is absent in human patients with central diabetes insipidus, and its presence is also dependent on age and individual variation.[26–29] In our study, the bright spot was visible in 6 of 11 dogs, representing a lower percentage, compared with previous studies[8–10] in healthy dogs. The absence of a bright spot is thus not indicative of pituitary neoplasia. The displacement of the bright spot seems to provide more reliable evidence of pituitary neoplasia. In fact, although slight variation in position was reported in healthy dogs,[10] the normal anatomic position of the bright spot in dogs seems to be located centrally in the midcaudal and dorsal portion of the pituitary gland.[8–10] In our study, the 2 dogs with a displaced bright spot had a bright spot still located in the midcaudal portion of the pituitary gland but displaced laterally and located off center. It can be speculated that the displacement of the bright spot on precontrast MR images can be interpreted in the same way as changes of the pituitary flush on dynamic CT images (ie, the result of a pituitary tumor) and thus provides important presurgical information regarding its location. In conclusion, results of our study indicated that dynamic CT and low-field MRI of the pituitary gland were equally diagnostic in the diagnosis of pituitary-dependent hyperadrenocorticism.

a. Philips Tomoscan CX/S, Philips NV, Eindhoven, The Netherlands.
b. Telebrix 350, Guerbet, Villepinte, France.
c. Magneton Open Viva, Siemens AG, Germany.
d. Dotarem, Guerbet, Villepinte, France.

References

1. van der Vlugt-Meijer RH, Meij BP, van den Ingh TS, et al. Dynamic computed tomography of the pituitary gland in dogs with pituitary-dependent hyperadrenocorticism. *J Vet Intern Med* 2003; 17:773–780.
2. van der Vlugt-Meijer RH, Meij BP, Voorhout G. Dynamic computed tomographic evaluation of the pituitary gland in healthy dogs. *Am J Vet Res* 2004;65:1518–1524.
3. van der Vlugt-Meijer RH, Meij BP, Voorhout G. Intraobserver and interobserver agreement, reproducibility, and accuracy of computed tomographic measurements of pituitary gland dimensions in healthy dogs. *Am J Vet Res* 2006;67:1750–1755.
4. van der Vlugt-Meijer RH, Voorhout G, Meij BP. Imaging of the pituitary gland in dogs with pituitary-dependent hyperadrenocorticism. *Mol Cell Endocrinol* 2002;197:81–87.
5. Kooistra HS, Voorhout G, Mol JA, et al. Correlation between impairment of glucocorticoid feedback and the size of the pituitary gland in dogs with pituitary-dependent hyperadrenocorticism. *J Endocrinol* 1997;152:387–394.
6. Meij BP, Voorhout G, van den Ingh TS, et al. Results of transsphenoidal hypophysectomy in 52 dogs with pituitary-dependent hyperadrenocorticism. *Vet Surg* 1998;27:246–261.
7. Meij BP, Voorhout G, Van den Ingh TS, et al. Transsphenoidal hypophysectomy in beagle dogs: evaluation of a microsurgical technique. *Vet Surg* 1997;26:295–309.
8. Graham JP, Roberts GD, Newell SM. Dynamic magnetic resonance imaging of the normal canine pituitary gland. *Vet Radiol Ultrasound* 2000;41:35–40.
9. Kippenes H, Gavin PR, Kraft SL, et al. Mensuration of the normal pituitary gland from magnetic resonance images in 96 dogs. *Vet Radiol Ultrasound* 2001;42:130–133.
10. van der Vlugt-Meijer RH, Meij BP, Voorhout G. Thin-slice three-dimensional gradient-echo magnetic resonance imaging of the pituitary gland in healthy dogs. *Am J Vet Res* 2006;67:1865–1872.
11. Bertoy EH, Feldman EC, Nelson RW, et al. Magnetic resonance imaging of the brain in dogs with recently diagnosed but untreated pituitary-dependent hyperadrenocorticism. *J Am Vet Med Assoc* 1995;206:651–656.
12. Duesberg CA, Feldman EC, Nelson RW, et al. Magnetic resonance imaging for diagnosis of pituitary macrotumors in dogs. *J Am Vet Med Assoc* 1995;206:657–662.
13. Guy RL, Benn JJ, Ayers AB, et al. A comparison of CT and MRI in the assessment of the pituitary and parasellar region. *Clin Radiol* 1991;43:156–161.
14. Johnson MR, Hoare RD, Cox T, et al. The evaluation of patients with a suspected pituitary microadenoma: computer tomography compared to magnetic resonance imaging. *Clin Endocrinol (Oxf)* 1992;36:335–338.
15. Hanson JM, van 't HM, Voorhout G, et al. Efficacy of transsphenoidal hypophysectomy in treatment of dogs with pituitary-dependent hyperadrenocorticism. *J Vet Intern Med* 2005;19:687–694.
16. Rijnberk A, van Wees A, Mol JA. Assessment of two tests for the diagnosis of canine hyperadrenocorticism. *Vet Rec* 1988;122: 178–180.

17. Stolp R, Rijnberk A, Meijer JC, et al. Urinary corticoids in the diagnosis of canine hyperadrenocorticism. *Res Vet Sci* 1983;34:141–144.
18. Meij B, Voorhout G, Rijnberk A. Progress in transsphenoidal hypophysectomy for treatment of pituitary-dependent hyperadrenocorticism in dogs and cats. *Mol Cell Endocrinol* 2002;197:89–96.
19. Hanson JM, Teske E, Voorhout G, et al. Prognostic factors for outcome after transsphenoidal hypophysectomy in dogs with pituitary-dependent hyperadrenocorticism. *J Neurosurg* 2007;107:830–840.
20. Bosje JT, Rijnberk A, Mol JA, et al. Plasma concentrations of ACTH precursors correlate with pituitary size and resistance to dexamethasone in dogs with pituitary-dependent hyperadrenocorticism. *Domest Anim Endocrinol* 2002;22:201–210.
21. Rijnberk A, Mol JA, Rothuizen J, et al. Circulating proopiomelanocortin-derived peptides in dogs with pituitary-dependent hyperadrenocorticism. *Front Horm Res* 1987;17:48–60.
22. Voorhout G, Rijnberk A, Sjollema BE, et al. Nephrotomography and ultrasonography for the localization of hyperfunctioning adrenocortical tumors in dogs. *Am J Vet Res* 1990;51:1280–1285.
23. Meij BP. Hypophysectomy as a treatment for canine and feline Cushing's disease. *Vet Clin North Am Small Anim Pract* 2001;31:1015–1041.
24. Bertoy EH, Feldman EC, Nelson RW, et al. One-year follow-up evaluation of magnetic resonance imaging of the brain in dogs with pituitary-dependent hyperadrenocorticism. *J Am Vet Med Assoc* 1996;208:1268–1273.
25. Kurokawa H, Fujisawa I, Nakano Y, et al. Posterior lobe of the pituitary gland: correlation between signal intensity on T1-weighted MR images and vasopressin concentration. *Radiology* 1998;207:79–83.
26. Brooks BS, el Gammal T, Allison JD, et al. Frequency and variation of the posterior pituitary bright signal on MR images. *Am J Neuroradiol* 1989;10:943–948.
27. Colombo N, Berry I, Kucharczyk J, et al. Posterior pituitary gland: appearance on MR images in normal and pathologic states. *Radiology* 1987;165:481–485.
28. Fujisawa I, Nishimura K, Asato R, et al. Posterior lobe of the pituitary in diabetes insipidus: MR findings. *J Comput Assist Tomogr* 1987;11:221–225.
29. Sato N, Ishizaka H, Matsumoto M, et al. MR detectability of posterior pituitary high signal and direction of frequency encoding gradient. *J Comput Assist Tomogr* 1991;15:355–358.